



## **A High Performance, Noncircular Tokamak Power Reactor Design Study - UWMAK-III**

**R.W. Conn, G.L. Kulcinski, C.W. Maynard, R.  
Aronstein, R.W. Boom, A. Bowles, R.G. Clemmer, J.  
Davis, G.A. Emmert, S. Ghose, Y. Gohar, J. Kesner, S.  
Kuo, E. Larsen, J. Scharer, I.N. Sviatoslavsky, D.K. Sze,  
W.F. Vogelsang, T.F. Yang, and W. Young**

**August 1976**

**UWFDM-168**

Published in the Proceedings of the Sixth IAEA Conference on Plasma Physics and  
Controlled Nuclear Fusion Research, Berchtesgaden, Federal Republic of Germany, 6-13  
October 1976.

***FUSION TECHNOLOGY INSTITUTE***

***UNIVERSITY OF WISCONSIN***

***MADISON WISCONSIN***

# **A High Performance, Noncircular Tokamak Power Reactor Design Study - UWMAK-III**

R.W. Conn, G.L. Kulcinski, C.W. Maynard, R.  
Aronstein, R.W. Boom, A. Bowles, R.G.  
Clemmer, J. Davis, G.A. Emmert, S. Ghose, Y.  
Gohar, J. Kesner, S. Kuo, E. Larsen, J. Scharer,  
I.N. Sviatoslavsky, D.K. Sze, W.F. Vogelsang, T.F.  
Yang, and W. Young

Fusion Technology Institute  
University of Wisconsin  
1500 Engineering Drive  
Madison, WI 53706

<http://fti.neep.wisc.edu>

August 1976

UWFDM-168

Published in the Proceedings of the Sixth IAEA Conference on Plasma Physics and Controlled Nuclear Fusion Research, Berchtesgaden, Federal Republic of Germany, 6-13 October 1976.

A High Performance, Noncircular Tokamak Power

Reactor Design Study - UWMAK-III

R. W. Conn, G. L. Kulcinski, C. W. Maynard, R. Aronstein\*,  
R. W. Boom, A. Bowles\*, R. G. Clemmer, J. Davis\*\*, G. A.  
Emmert, S. Ghose\*, Y. Gohar, J. Kesner, S. Kuo\*\*\*, E. Larsen,  
J. Scharer, I. Sviatoslavsky, D. K. Sze, W. F. Vogelsang,  
T. F. Yang, W. D. Young

August, 1976

Fusion Technology Program  
Nuclear Engineering Department  
University of Wisconsin  
Madison, Wisconsin  
United States of America

UWFDM-168

\* Bechtel Corporation, San Francisco, CA  
\*\* McDonnell-Douglas Astronautics Co.- East, St. Louis, MO  
\*\*\* United Technologies Research Center, East Hartford, CT

Published in the Proceedings of the Sixth IAEA  
Conference on Plasma Physics and Controlled Nuclear Fusion Research,  
Berchtesgaden, West Germany, October 6-13, 1976

## "LEGAL NOTICE"

"This work was prepared by the University of Wisconsin as an account of work sponsored by the Electric Power Research Institute, Inc. ("EPRI"). Neither EPRI, members of EPRI, the University of Wisconsin, nor any person acting on behalf of either:

"a. Makes any warranty or representation, express or implied, with respect to the accuracy, completeness, or usefulness of the information contained in this report, or that the use of any information, apparatus, method, or process disclosed in this report may not infringe privately owned rights; or

"b. Assumes any liabilities with respect to the use of, or for damages resulting from the use of, any information, apparatus, method or process disclosed in this report."

A HIGH PERFORMANCE, NONCIRCULAR TOKAMAK POWER  
REACTOR DESIGN STUDY - UWMAK-III

R. W. CONN, G. L. KULCINSKI, C. W. MAYNARD, R. ARONSTEIN<sup>(\*)</sup>, R. W. BOOM,  
A. BOWLES<sup>(\*)</sup>, R. G. CLEMMER, J. DAVIS<sup>(\*\*)</sup>, G. A. EMMERT, S. GHOSE<sup>(\*)</sup>,  
Y. GOHAR, J. KESNER, S. KUO<sup>(\*\*\*)</sup>, E. LARSEN, J. SCHARER, I. SVIATOSLAVSKY,  
D. K. SZE, W. F. VOGELSANG, T. F. YANG, W. D. YOUNG

Fusion Technology Program, Nuclear Engineering Dept.  
The University of Wisconsin, Madison, Wis., U.S.A.

Abstract

UWMAK-III is a conceptual power reactor design study aimed at understanding the problems associated with using advanced technologies and several new or different design approaches in tokamak systems. Advanced technologies studied include the use of the molybdenum based alloy, TZM, as the primary structural material, the use of aluminum as the stabilizer and aluminum alloy structure for the NbTi superconducting magnets, and the use of a closed cycle helium gas turbine power conversion system. New or different design approaches include the study of RF (fast magnetosonic waves) plasma heating, a blanket design where tritium breeding is accomplished only in the outer blanket region, a permanent inner blanket that is basically a hot shield, tritium extraction and recycling processes, and the general design approach to blanket module removal. The maximum module weight is only 42 t. An MHD analysis has determined the noncircular plasma shaped as a characteristic "D" with neutral points on the plasma boundary for a poloidal divertor. The reactor is small (major radius = 8.1 m) with a relatively high  $\beta$  (about 9%), and an average neutron wall loading of 2.5 MW/m<sup>2</sup>. It is designed to generate 5000 MW(th) during the burn and 1985 MW(e) continuously. The net plant efficiency is about 42%. Aspects of the design study discussed in some detail include the plasma physics analysis, magnet design, blanket and shield neutronic and thermal analyses, tritium extraction, materials performance, and radiation damage. A brief discussion is included on the questions of size and costs in tokamak systems and their approximate relation with other advanced power generating technologies.

---

(\*) Bechtel Corporation, San Francisco, Calif.

(\*\*) McDonnell-Douglas Astronautics Co.-East, St. Louis, Mo.

(\*\*\*) United Technologies Research Center, East Hartford, Conn.

## 1. Introduction

UWMAK-III is a conceptual power reactor design study of a noncircular tokamak with the aim of assessing the prospects and problems associated with utilizing several advanced technologies in a tokamak reactor system. The reactor is designed to produce the same thermal power output, 5000 MW, as our earlier studies, UWMAK-I [1,2] and UWMAK-II [3,4] but it is considerably smaller in physical size. The major parameters characterizing the reactor are listed in Table 1 and an enlarged cross section view of the main reactor island is shown in Fig. 1. An overall view of the plant design showing the layout of necessary buildings is given in Fig. 2. The reactor is designed to produce a continuous net electrical output of 1985 MW with a net plant efficiency of 41.9%.

Before discussing the design study in detail, it is worth enumerating several of the important features and unique aspects of UWMAK-III.

(1) UWMAK-III is substantially reduced in size compared to our earlier studies [1-4]. A comparison of the plasma and toroidal field magnet size and shape between UWMAK-II [3,4] and UWMAK-III is shown in Fig. 3. The size reduction is primarily the result of utilizing a high plasma beta ( $\sim 9\%$ ) and an average 14 MeV neutron wall loading of about  $2.5 \text{ MW/m}^2$ .

(2) A high beta "D" shaped plasma has been designed based on two dimensional MHD equilibrium studies which show that such plasma equilibria can be found even with discrete external coils located far from the plasma (outside the blanket and shield) and with null points on the plasma boundary.

(3) RF heating has been studied to assess its potential for heating reactor plasmas to ignition conditions [5]. After an initial assessment of various wave heating modes, our efforts were concentrated on the fast magnetosonic wave [6] because of its direct heating of the ions, its accessibility and apparent penetration to the plasma core, and the potential for generating large amounts of RF power at the required frequency (about 60 MHz).

(4) The NbTi superconducting magnet design utilizes an aluminum stabilizer with high strength aluminum alloy as its structure. In addition to cost advantages, this allows for compatible contraction of both the conductor and the structure on cool down or warm up, and reduced activation by neutrons.

(5) The molybdenum based alloy, TZM (99.4% Mo, 0.5% Ti, 0.08% Zr, 0.01% C), is chosen as the primary structural material because of the desire to increase the operating temperature of the coolant while using a material which, unlike vanadium or niobium alloys, is compatible with both helium or liquid lithium coolants. This particular alloy shows a high resistance to radiation damage from neutrons. In addition, the U.S. has a good resource position with respect to Mo.

(6) The blanket design is unique in that tritium breeding takes place only in modules on the outer portion of the torus. A schematic illustration is given in Fig. 4. In the outer blanket, liquid lithium is used as both the coolant and breeder material. The pumping problems are minimized by good access and low magnetic field. The inner blanket nearest the torus centerline is not designed to breed tritium and its first structural wall is protected from radiation damage by a graphite neutron spectral shifter or ISSEC [7]. Thus, the inner blanket is designed as a hot shield and is expected to last for the life of the plant. The outer blanket module will be damaged by radiation and will have to be removed periodically (approximately once every

two years). A highly modularized outer blanket design has been developed in which the largest element that must be moved weighs 42 t.

(7) The blanket neutronics analysis has been carried out using two dimensional neutron and photon transport in toroidal geometry. This is found to be especially important when the blanket design is not poloidally symmetric. The major radius,  $R$ , and the height above the midplane,  $Z$ , are used as the main coordinates. Symmetry is assumed in the toroidal angle,  $\phi$ . Existing cylindrical geometry transport codes have been adopted to successfully complete the toroidal neutronics analysis.

(8) A closed cycle helium gas turbine power conversion system has been designed and studied. The helium coolant from the inner blanket goes directly to a helium turbine while the lithium from the outer blanket goes to a Li-Na intermediate heat exchanger. Sodium from the intermediate loop plays the triple role of isolating the tritium containing lithium from the power cycle, providing a working fluid for thermal energy storage, and protecting the primary structure from high pressures in the event of a leak in a heat exchanger. Thermal storage is required to level the electrical output from the turbines despite the pulsed nature of the tokamak burn cycle.

(9) The plant layout and building design shown in Fig. 2 has produced a compact system design. The primary containment building is, within 20%, the same size as that designed for the 350 MWe Clinch River Breeder Reactor, a demonstration LMFBR [8], and the overall plant size is likewise about the same.

(10) An assessment is made of the materials resource implication of a UWMAK-III type power reactor economy. The most serious problems appear to be associated with the expansion of an established industry rather than the question of sufficient resources.

(11) An economic study has been carried out in collaboration with the Bechtel Corporation using a macro composite systems approach in an effort to identify key cost areas in tokamak fusion systems. The resulting estimates have been compared with estimates developed by Bechtel for other advanced, non-fuel-limited approaches to electric power generation.

We summarize in this paper details relating particularly to the plasma analysis, blanket and shield design, materials, tritium, overall plant design and system economics. The design of the toroidal field magnet system has been given by Boom, Moses and Young [9] and the analysis of the power cycle is described by Conn and Kuo [10] in other publications. A much more extensive discussion on all aspects of the UWMAK-III study is given in reference 11.

## 2. Plasma Design and Analysis

Noncircular plasma cross sections offer the potential for achieving higher plasma  $\beta$  values compared to circular plasmas of equal poloidal beta,  $\beta_\theta$ , or safety factor,  $q$  [12]. The scaling is

$$\beta = \beta_\theta \left( \frac{S}{qA} \right)^2$$

where  $A$  is the aspect ratio and  $S$  is the plasma shape factor. Therefore, a detailed MHD equilibrium study has been carried out to determine the plasma shape shown in Fig. 1. The code used to perform this analysis was developed by the MHD group at Princeton [13]. The plasma has been satisfactorily tested for stability against rigid displacements and localized interchange

modes. The large triangularity of the shape is the result of forcing the vacuum vertical field to have good curvature.

The plasma burn cycle is summarized in Table 2. An air core transformer with superconducting windings located as shown on Fig. 1 is designed to bring the plasma current up linearly from some nominal value to the operating level of 15.8 MA. The vertical or equilibrium field coils actually provide approximately 96% of the startup flux with the OH windings providing the rest. The total flux swing during the current rise phase is 254 V-s. The flux swing required during the 15 second plasma heating phase and the 30 minute burn is provided by the OH windings alone. The flux swing required, based on a general expression for the plasma electrical conductivity including particle trapping and impurity effects, is 107 V-s. The peak power requirement is 913 MW during the current rise phase and is assumed to be provided by 500 MW off the line and the rest from an inductive energy storage unit similar to that designed for UWMAK-II [3,4].

The plasma reaches a temperature of only 1.8 keV during the ohmic heating phase. Thus, auxiliary heating is required to ignite the plasma and bring it to its steady state operating condition during the burn period. RF heating has been examined for this purpose and the fast magnetosonic wave at  $\omega = 2\omega_{CD}$  has been studied in detail. Analysis shows that the ion cyclotron harmonic absorption term occurs in a vertical band of finite width,  $\Delta$ , centered at the plasma major radius. The finite width is less than the plasma radius and is due to thermal effects and the  $1/R$  variation of the toroidal field, where  $R$  is the major radius. The energy deposited in this slab is then uniformly distributed over the flux surfaces due to the rotational transform. The expression for the ion heating profile is directly proportional to  $R/r$ , where  $r$  is the local plasma radius, and is therefore strongly peaked at the plasma center.

The existence of toroidal eigenmodes [6] also has a strong effect. In smaller devices, these eigenmodes are well separated but in large reactor systems like UWMAK-III, the density of toroidal eigenmodes in frequency domain becomes a near continuum [5]. This means the eigenmodes will always be available to heat the plasma, but the cumulative effect of all excited modes on the loading of the launching structure and on the heating efficiency is a subject requiring further research.

The theoretical expression for plasma ion heating by the fast magnetosonic wave is used together with a global model of plasma behavior [14,5] to analyze the heatup rate. At the end of the 15 s ohmic heating phase, 40 MW of RF wave heating at 60 MHz is turned on. After 8 s, the plasma reaches ignition and if the RF power is left on for 12 s, the plasma reaches the equilibrium temperature of  $T_i \approx 19$  keV,  $T_e \approx 23$  keV after 15 s. An alternative scenario was also studied in which 200 MW of injected RF is used to rapidly heat the plasma past ignition and then allow alpha heating to take over. This would be an interesting scenario if the plasma can be operated in the "flux conserving" mode [15].

An important problem with RF heating, in addition to adequate coupling of the waves to the plasma, is the design of a suitable launching structure located on the torus wall. It must be capable of handling 200 MW of power



at 60 MHz for a startup period of up to 15 seconds, and it must be designed for the excitation of modes that lead to energy deposition near the plasma core.

An ideal system would have a spectrum which excites lower order poloidal  $m$  values. Higher order  $m$  values cause the finite ion gyroradius heating to peak further towards the plasma edge, leading to edge heating rather than core heating. In order to excite only low  $m$  numbers, the source distribution would have to cover most of the poloidal circumference. A further problem is caused by the fact that for large tokamaks such as UWMAK-III, the minor circumference is large compared to a free space wavelength. This introduces phase shifts of a wave traveling in the poloidal direction which can contribute to a higher order poloidal spectrum and reduce the efficiency. This may be overcome by introducing external circuit phase shifts which correct for the natural phase shift of the wave as it travels in the poloidal sense.

A standard rectangular waveguide launcher flush mounted in the wall introduces a new spectral excitation problem since its toroidal dimension must be larger than half a free space wavelength for propagation of the dominant  $TE_{10}$  mode. This can be overcome by using smaller waveguides, possibly filled with the high dielectric ceramic which reduces the dimension of the guide and excites larger  $k_{11}$  values. If the radiation damage and high temperatures introduced into the ceramic can be tolerated, a strip line located over a ceramic dielectric inside a rectangular guide could be envisioned which does not have a cut-off limitation due to small aperture size. The conducting strip would have to be coupled to the torus by making a small loop which is electrically connected to the bottom of the guide.

For the design used in UWMAK-III, a ridged waveguide has been considered in order to reduce the toroidal extent of the guide for improved wave penetration and heating. This reduces the mode conversion potential and provides a means of determining the fraction of wave power initially deposited in the ions. The H-shaped guide would have the inner dimensions of 1 m high by 1 m wide with a gap width of 8.7 cm which is 50 cm in extent. The wave impedance of the dominant  $TE_{10}$  mode is 70 ohms and the theoretical power carrying capability is 30 MW.

If neutron and plasma heating of the guide aperture are not too severe, a guide which is partially or fully filled with a dielectric medium can be considered. A ridged waveguide which is filled with alumina can be designed which is 50 cm wide by 50 cm high with a 10 cm gap. The wave impedance is 40 ohms and a theoretical power transfer of 60 MW can be obtained.

It is evident that several alternatives for the design of magnetosonic wave launching structures exist. From purely a plasma point of view, a wave source distribution is proposed that goes half way around the minor cross section on the outside edge. A second source located very close to the first but shifted in phase by  $180^\circ$  is proposed in order to set up short wavelengths ( $\lambda = 1m$ ) in the toroidal sense. This approach however presents some obvious problems with regard to the placement of the vertical field coil and to access. The added complexity led to the design approach shown in Fig. 1. This design was used as the basis for locating the equilibrium vertical field coils used in the MHD analysis described earlier.

The equilibrium plasma conditions during the plasma burn for UWMAK-III have been studied by using both a global plasma energy balance model [14] and a more sophisticated space-time tokamak code [16]. In both cases, thermal equilibria are found which produce 5000 MW<sub>th</sub> of power. In the latter case, however, the average ion and electron temperatures, the plasma  $\beta_0$ , and the particle confinement time are found to be significantly lower than those predicted by the global model because the temperature and density profiles are sharply peaked at the axis of the torus.

The plasma and magnetic field parameters are listed in Table 1b-d. The energy confinement time is 1.6 sec while the particle confinement time is 0.55 sec. The fractional burnup is very low, 0.83%, and the fueling rate for D plus T atoms is  $1.43 \times 10^{21}$ /sec. This low fractional burnup and correspondingly high fueling rate results because the diffusion of particles from the plasma is governed by the diffusion coefficient at the plasma edge. The edge condition associated with the use of an unload divertor implies a very low density and therefore a quite collisionless plasma. In turn, this leads to a large diffusion coefficient assuming microinstability scaling [17]. The low value of  $\tau_p$  in the space dependent model means the amount of tritium in the refueling cycle will be much larger than heretofore expected on the basis of global model calculations alone. In this case, the fueling rate for tritium is 74.7 kg/day.

Two forms of impurity control are included in the UWMAK-III design, a magnetic divertor and a low Z liner. The magnetic divertor is of the axisymmetric, poloidal double null type such as we have used previously [1-4]. The low Z liner consists of a thick graphite zone (25 cm) on the inner portion of the chamber nearest the centerline and a thin carbon curtain [18], as described in UWMAK-II [3-4], mounted on the outer blanket first wall. The operation of the carbon curtain is similar to that described previously and the temperature during the plasma burn is 1300°C. As such, physical sputtering is expected to dominate. The thick graphite zone on the inner side of the chamber will operate with a much higher surface temperature in the neighborhood of 1800°C. The erosion rate will be governed by physical sputtering and the "possible" formation of acetylene. Low energy atomic hydrogen studies show effective yield coefficients of 1 to  $3 \times 10^{-3}$  [19]. If these values do not increase by more than a factor of 10 at 10-30 keV, then the erosion of the ISSEC will be manageable.

The effectiveness of the divertor in reducing the charged particle flux to the wall has been estimated using the model described previously [4]. The design of the divertor in UWMAK-III is unique in several ways. Firstly, the particles bombard a thin, solid plate of TZM located outside the toroidal field magnets and the pumping and heat transfer problems are not coupled (see Fig. 1). Placing the bombardment plates outside the TF coils allows the field lines to be fanned out, thus reducing the power density of particles on the plates. Combining this with the relatively small flow conductance back through the slots to the plasma, one expects that there will be little backstreaming of neutrals and impurities.

A pumping scheme for a fusion reactor is complicated by the fact that twice as many pumps as needed in normal operation have to be provided to

allow one half of them to be recycled while the outer half are on line. This implies low conductance gate valves, heaters, backup pumps and many ducts and vacuum lines. Nevertheless, a system such as UWMAK-III lends itself to a reasonably simple design. We envisage that all pumping of the main chamber will be by cryopumps that are rectangular in shape and will cover about 65% of the available area in the particle collection chamber. The total pumping area will be  $1600 \text{ m}^2$ , with only one half of the pumps in use at one time and the pumps would be regenerated every five hours. (Time between regenerations can be as little as 2.5 hours.)

### 3. Magnet System Design

The design analysis for the UWMAK toroidal field magnets is given elsewhere [9]. To summarize briefly, the toroidal field coils for UWMAK-III shown in Fig. 1 have a modified constant tension "D" shape, corrected for the field variation due to the finite number (18) of coils. The embedded conductor in a solid "D" shaped alloy aluminum former is used to minimize the material requirements while providing maximum strength and stiffness. This construction was described in detail in the UWMAK-I report [1] and the cold central structure and secondary vacuum wall used in the UWMAK-II [3] design are retained. The superconductor is TiNb superconducting filaments processed in an OFHC copper matrix for convenience but stabilized with high-purity aluminum in the case of the toroidal field magnets. The coils are fully cryogenically stabilized and produce a maximum field of 8.75 T and an axial field at  $R = 8.1 \text{ m}$  of 4.05 T. The smaller size of UWMAK-III has also led to a sharp reduction in the TF coils size. As one measure, we note that the stored energy in the toroidal field of UWMAK-III is 108 GJ compared with 216 GJ in the UWMAK-II design.

A unique feature of the UWMAK-III TF coils is the use of an Al conductor and an Al alloy structure. The use of 316 stainless steel for the structural material in the toroidal field magnets in the UWMAK-I and UWMAK-II designs was predicated on a limiting maximum strain of 0.002 in the copper stabilizer and a desired high stress level to minimize structural volume. Recent work on alloy aluminum reinforced high purity aluminum stabilizers at the University of Wisconsin-Madison by H. Segal [20] leads to the possibility of cycling the high purity aluminum stabilizer to a strain level of 0.0038 with little degradation in its resistivity ratio.

The advantages of using aluminum as the stabilizer and high strength aluminum alloy as the structure, compared with copper and steel, include lower resistivity, lower weight and cost, easier fabrication, compatible thermal expansion and contraction, lower heat capacity (for cool down) and lower activation by the small, but finite flux of neutrons leaking from the shield. Some disadvantages include lower design stresses, somewhat larger size, and lower heat capacity (for thermal accidents). The potential benefits are clear and further investigations here are clearly suggested.

### 4. Blanket and Shield Design

A schematic illustration of the blanket and shield design in UWMAK-III is given in Fig. 4 and the philosophy behind this design was given in section 1. A detailed two dimensional toroidal geometry neutronics and photonics analysis

has been completed to determine the nuclear performance of the system [21]. The results are given in Table 1c. An important point to note is that the neutron wall loading is not uniform and this leads to poloidal variations in heating rates and radiation damage which have been included in the thermal hydraulics and materials studies. The wall loading variation as a function of poloidal angle is shown in Fig. 5a.

From a heat transfer viewpoint, the blanket and shield design in Fig. 4 has three distinct components: the hot inner shield, the partial ISSEC zone, and the outer breeding blanket. The heat deposited in the ISSEC zone will be transported to the front and back surfaces of the graphite and radiated away. The analysis indicates that the maximum temperature occurs inside the graphite and is less than 2000°C, assuming the thermal conductivity is degraded similar to nuclear grade material. The surface temperature facing the plasma is somewhat less than the maximum (~1800°C).

The outer blanket is designed to give the lowest value of  $\mathbf{v} \times \mathbf{B}$  and minimizes MHD effects. Problems of thermal recirculation within a cell are solved by the use of a 10 cm wide static lithium zone in the middle of the cell for thermal insulation. (The lithium velocity in this buffer zone is sufficient for tritium recovery). The maximum coolant pressure on the first wall is only 70 psia and the pumping power required is just 2 MW. The maximum temperature of the TZM structure is 1000°C and the lithium exit temperature is 980°C.

The inner hot shield, or inner blanket, is cooled with helium. A 0.5 m diameter feed tube is introduced between the TF magnets and connected to a manifold running in the toroidal direction. The surface heating load on the inner blanket is 35 W/cm<sup>2</sup> and, together with the space dependent volumetric heating from the neutronics analysis, leads to a coolant inlet temperature of 488°C and an outlet temperature of 870°C at 1000 psia pressure. These coolant conditions match the temperature of the helium coming from the secondary heat exchanger of the outer blanket cycle such that identical turbines and thermal energy storage can be used. The distribution of coolant tubes within the inner blanket is arranged to be inversely proportional to the heating rate so that the heat load on each coolant is approximately the same.

The blanket cells are approximately 2 m x 2.2 m and the entire outer blanket (which is the part which must be removed because of radiation damage) is built up from these basic modules. The heaviest module which would have to be removed weighs just 42 MT and a sequence of steps have been devised for such a process. The outer shield is designed to swing open so that only blanket module removal would be required.

## 5. Tritium System Analysis

Extensive details on the tritium systems for both UWMAK-II and UWMAK-III have been given recently by Clemmer, Larsen and Wittenberg [22]. We, therefore, restrict the discussion here to the problem of removing tritium from the liquid lithium breeder.

Tritium is extracted by diverting about 5% of the liquid lithium in the

outer blanket to a niobium window. Niobium is particularly well suited for this purpose because it has a high permeability to hydrogen at these temperatures and it allows us to reduce the tritium concentration in the lithium to a level compatible with subsequent tritium losses to the environment. Other methods for the extraction of tritium from lithium, such as yttrium beds, molten salt extraction, liquid alloy getters and fractional distillation, were considered but were not found to be as attractive.

However, the niobium window is not without its own problems. The oxygen level in the niobium must be less than 100 ppm or the lithium will erode the surface, even going up grain boundaries to react with oxygen. Also carbon transport from the TZM will occur, causing embrittlement of the niobium. In addition, at 980°C, niobium will be subject to attack by the oxygen getter in the helium stream and therefore some protective barrier is required. Palladium is the barrier of choice since it has a high hydrogen permeability. A palladium thickness of 0.001 cm deposited by electrodeposition will give a coherent layer of suitable durability. This will require a total of 170 kg of palladium for the calculated surface area of the window. However, the mutual solubility of Nb and Pd is high and it is expected that the palladium will diffuse into the niobium though no firm data exists for the rates of interdiffusion. Therefore, an intermediate yttrium layer is proposed which should minimize the rates of diffusion so that a practical "window" lifetime can be achieved. Yttrium was chosen because it, along with other IIIa elements and some of the rare earth metals, is among the few metals which does not form solid solutions with niobium. The required yttrium layer thickness is estimated to be 2500 Å. This will require a total of 2.0 kg of this element for the calculated surface area of the window. Experimental work is thus required to establish that Nb windows appropriately protected can be operated reliably.

Another important aspect of high temperature operation in general is that large amounts of tritium could leak through pipes. For example, the high temperature side of the lithium system is at 980°C and has a tritium pressure of  $1.0 \times 10^{-6}$  torr. The approximate pipe dimensions are  $2 \times 10^6 \text{ cm}^2$  and 5 mm thickness. Assuming the downstream pressure is zero, the leak through such piping is 92 curies per day. However, to protect the TZM from oxidation, the pipe is double walled using the outer pipe of stainless steel lined with ceramic insulating material. Since the temperature of the jacket is much lower and the permeability of the ceramic is very low, the release of tritium to the reactor is vanishingly small. However, such double walled pipe is expensive and may be a factor in the ultimate usability of high temperature materials.

The overall plant inventory of tritium is estimated to be 35.8 kg. It should be noted that of this only 1.7 kg is in the breeding-recovery cycle. The 34.1 kg in the refueling cycle includes 18.6 kg in reserve storage. The reason the refueling cycle inventory is so large is the small particle confinement time predicted by space-time analysis of plasma performance. The result is a fractional tritium burnup of only 0.8%.

Assuming 5% burnup, the refueling cycle tritium inventory would only be 5.5 kg and the total plant inventory would be 7.2 kg.

## 6. Radiation Effects Analysis

The radiation damage environment in UWMAK-III is much more severe than in previous UWMAK reactors because of the smaller size. The maximum wall loading is  $\sim 3.5 \text{ MW/m}^2$  and the average value is  $\sim 2.5 \text{ MW/m}^2$ . (Fig. 5a). When the back scattered neutrons are considered, the displacement and helium production rates in the TZM first walls vary in the poloidal direction as shown in Fig. 5b. The maximum dpa rate is  $\sim 19 \text{ dpa/yr}$  (100% plant factor (P.F.)) in the outer blanket and  $3.5 \text{ dpa/yr}$  behind the ISSEC shield. The associated helium production rates are  $120 \text{ appm/yr}$  and  $\sim 13 \text{ appm/yr}$  at 100% P.F. Extrapolation of this data to present fission neutron and charged particle simulation studies is difficult because of the lack of data. Preliminary analysis reveals that the outer first wall lifetime is likely to be greater than 6 years for 10% swelling in TZM and the inner TZM walls will not achieve this value in 30 years. There have been no studies with such large amounts of helium in TZM, but again, preliminary analysis reveals that helium levels in the 10-25 appm range actually increase the fatigue and creep life of Mo and TZM after irradiation [23,24]. To be conservative, we have limited the outer TZM wall lifetime to the time required to accumulate 200 appm helium. This criteria requires that some parts of the walls be replaced every 1.5 to 2 years. The electrical resistance increase in the walls of the RF waveguides has been found to be less than 3% per year. Since the lifetime of the modules is 1.5 to 3 years, this increase should represent no particular problem.

The radiation damage to the carbon curtain has been analyzed with reference to current dimensional stability data on reactor grade graphites. The analysis reveals that the curtain will last at least 3 years at  $1300^\circ\text{C}$ . The situation with respect to the ISSEC is more uncertain. The large majority of data indicates that as the irradiation temperature increases from  $1000$  to  $1400^\circ\text{C}$ , the amount of residual damage decreases [25]. Hence, we expect longer lifetimes (from a swelling standpoint) at  $2000^\circ\text{C}$  than at  $1400^\circ\text{C}$ . An exact value cannot be given now, but sputtering and vaporization are likely to limit the lifetime to 5 years and hence we have used that value for the lifetime of the ISSEC.

Radiation damage to the superconducting magnets has been analyzed and, aside from a few unique areas which are bombarded by neutrons leaking down divertor slots, there are no severe problems. Periodic annealing of the TF coil ( $\sim$  every 10 years) to room temperature should allow the Al stabilizer to maintain low  $I^2R$  losses (less than 10% over normal) in the event of an accident. The degradation of the critical superconducting properties of the TiNb is less than 10% over the plant lifetime.

Finally, analysis of the  $\text{B}_4\text{C}$ , 316 stainless steel and Pb in the shield plus mylar and organic insulation in the TF coils revealed no insuperable problems.

## 7. Plant Design and Building Size

The major features of the plant arrangement shown in Fig. 2 include the following: the containment building is centrally located relative to the outer building. It is a reinforced concrete structure lined with stainless steel and it has an inert environment to prevent lithium or sodium fire. The heat exchanger building, radwaste building, auxiliary building, hot cell and the maintenance building are arranged around the containment building. This arrangement makes the plant layout very compact, with maximum utilization of space around the containment, by locating the reactor support systems and facilities close to the nuclear island. This is also expected to offer some economic advantages for piping, cabling and structural considerations. The peninsular arrangement of the Turbine Building orients the axes of the turbine-generators such that any missiles generated by the machines will not strike the containment building.

It is important to note that reducing the size of the nuclear island has produced a concomitant reduction in overall plant size. A perspective on this matter can be obtained by comparing the plant layout for UWMAK-III with that developed for the Clinch River fission breeder reactor (CRBR) [8]. The UWMAK-III systems occupies (not fully) a space 195 m by 138 m. The comparable set of structures for CRBR fits in a space that is 234 m by 159 m. The primary containment building for UWMAK-III is 70 m in diameter by 70 m high whereas the comparable CRBR containment building has a 60 m diameter and is 80.5 high. Only the turbine building in UWMAK-III is significantly larger and this is because the design electrical output is 1985 MW<sub>e</sub> compared to 350 MW for CRBR. Thus, tokamak reactors designed with the major characteristics<sup>e</sup> of UWMAK-III (size and shape) will be similar in size to advanced fission reactors, and not appreciably larger.

## 8. Economic Analysis

An economic analysis for UWMAK-III has been carried out to determine the major cost areas and to indicate where further research effort can yield the greatest cost benefit. It will only be possible to highlight key results here and the reader is referred to reference 11 for the in-depth analysis.

The estimate of direct field cost for UWMAK-III in 4th quarter 1975 dollars is \$1154/kWe broken down as follows: land and land rights, \$0.5/kWe; structures and site facilities, \$285/kWe; reactor plant equipment, \$408/kWe; turbine plant equipment, \$285/kWe; electric plant equipment, \$141/kWe; and miscellaneous plant equipment and special materials, \$34/kWe. Direct costs are most easily described since all other costs are derived as percentages thereof. Following Bechtel cost procedures, indirect costs add an additional \$986/kWe and owner costs and interest during construction add a final \$730/kWe. Note that the percentages applied for indirect costs to UWMAK-III are much higher than in earlier studies [1,3,26].

An analysis of costs by category led to the unanticipated result that the costs of high temperature refractory metal piping is critical while the costs of the toroidal field magnet system is relatively less important.

The piping costs were high because it is necessary to protect refractory metals from the atmosphere to avoid oxide formation and hydrogen embrittlement. Importantly, this is a general characteristic of all refractory metals (i.e. Nb, V, Ta) and is not specific to the use of molybdenum based alloys. The cost estimate developed for such pipe in the primary system is approximately \$10,700/m. As such, about a quarter of the nuclear island costs and about a third of the closed cycle helium turbine plant equipment costs were for the piping. It will be of great interest to redesign UWMAK-III (a relatively small unit physically with  $R = 8m$ ) using a lower technology structural material such as 316 stainless steel. Clearly, the absolute costs will be reduced significantly. It will be important to determine how much the associated reduction of net efficiency affects the net power costs.

An important auxiliary result is the breakdown by major category of the direct costs: 25% for buildings, 35% for the reactor plant equipment (nuclear island), 25% for the turbine plant, 12% for the electric plant equipment, and 3% for remaining miscellaneous items. Therefore, the nuclear island is 35% of the direct costs while the balance of plant is 65%. The toroidal field magnets were estimated to be 10% of the reactor plant equipment costs or just 3.5% of the total direct costs. This is much lower than anticipated and leads us to conclude that one can afford to pay more for higher magnetic field.

This result may have some very important implications. In particular, it can have an impact on the size of tokamak reactors. There are two reasons one would make a tokamak large. The first is to improve the confinement time of the plasma and the second is to keep the neutron wall loading to a prescribed but low value. A wall loading constraint at some level (high or low) is applicable to all magnetic approaches to fusion and is not specific to tokamaks. On the other hand, increasing the size to improve confinement time is more peculiar to closed line devices like tokamaks than it is to an open ended system like a mirror machine. However, almost all theories, as well as experience, indicate that the confinement time improves with magnetic field. Therefore, within a given wall loading constraint, tokamaks can be made as small as possible by increasing the magnetic field. The cost penalty on the coils will not be overwhelming whereas keeping the size small will lower the costs of buildings, piping, blanket systems and so on.

A perspective on UWMAK-III costs is provided in Fig. 6 where we plot the range of costs developed by the Bechtel Corp. for other advanced, non-fuel-limited, power generating sources. Also shown are costs for present day light water reactors (LWR's) and coal fired steam plants. Escalation costs are not included and net costs are given for the liquid metal fast breeder (LMFBR) reactor because no Bechtel developed costs were available. However, as a general gage, we note that the cost estimate for the Superphenix 1200 MWe commercial prototype LMFBR is about twice LWR costs or 45-50 mills/kwh. The likely range for commercial LMFBR's is 30-50 mills/kwh.

The perspective provided by Fig. 6 is that the estimated cost of a system like UWMAK-III appears to be comparable with estimates developed by Bechtel for other advanced energy power systems that are not fuel limited. Only solar



energy costs are well above all others.

Finally, we note that fusion reactor research is still at an early stage, that much inventiveness has already been shown, that there are many remaining directions for improving system design, (higher  $\beta$  [15], blanket designs for extended life at reduced size [27], new and positive information on radiation damage at lower temperatures in stainless steel [28], etc.) and that there is a critical need for new energy sources. Cost estimates at this stage are a guide and we are greatly encouraged to continue on with such studies.

Acknowledgement: This research was supported by the Electric Power Research Institute, Palo Alto, California.

#### References

- [1] BADGER, B. et al., "UWMAK-I, A Wisconsin Toroidal Fusion Reactor Design," Nucl. Eng. Dept. Report UWFD-68 (University of Wisconsin, Madison), Vol. 1 (1974), Vol. II (1975).
- [2] KULCINSKI, G. L. and CONN, R. W., in Fusion Reactor Design Problems (IAEA, Vienna, 1974) p. 51.
- [3] BADGER, B. et al., "UWMAK-II, A Conceptual Tokamak Power Reactor Design," Nucl. Eng. Dept. Report UWFD-112 (University of Wisconsin, 1975).
- [4] Plasma Physics and Controlled Nuclear Fusion Research 1974 (Tokyo Conf., IAEA, Vienna, 1975). See paper by R. W. Conn et al., Vol. III, p.497.
- [5] SCHARER, J., CONN, R. W., BLACKFIELD, D., "Study of RF and Neutral Beam Heating in Tokamak Reactors," Nucl. Eng. Dept. Report UWFD-148 (Univ. of Wisconsin, 1976).
- [6] ADAM, J. et al., in ref. 4, Vol. I, p. 65.
- [7] CONN, R. W., KULCINSKI, G. L., AVCI, H. and EL-MAGHRABI, M. Nucl. Technol. 26, 125 (1975).
- [8] JACOBI, W. M., "Design of Clinch River Breeder Reactor and Selection of Basic Plant Parameters," in J. M. Kallfelz and R. A. Karam, eds. Advanced Reactors: Physics, Design and Economics (Pergamon Press, Oxford, 1975.)
- [9] BOOM, R. W., MOSES, R. and YOUNG, W., Nucl. Eng. and Design, (1976) (in press).
- [10] CONN, R. W. and KUO, S., Nucl. Eng. and Design, (1976) (in press).
- [11] BADGER, B., et al., "UWMAK-III, A Conceptual Noncircular Tokamak Power Reactor Design" Nucl. Eng. Dept. Report UWFD-150 (Univ. of Wisconsin, 1976).

- [12] OHKAWA, T., VOORHIES, H. G., Phys. Rev. Letts. 22, 1275 (1969).
- [13] CHANCE, M. S. et al., in ref. 4, Vol. I, p. 463.
- [14] CONN, R. W., KESNER, J., Nucl. Fusion 15, 775 (1975).
- [15] CLARKE, J., "High Beta Flux Conserving Tokamak," ORNL-TM-5429 (1976).
- [16] HOGAN, J., Meth. Comp. Phys. 16, (1975).
- [17] KADOMTSEV, B.B., POGUTSE, O. P., in L. A. Leontovich, ed., Reviews of Plasma Physics (Consultants Bureau, N. Y. 1970). Vol. 5.
- [18] KULCINSKI, G. L., CONN, R. W., LANG, G., Nucl. Fusion 15, 327 (1975).
- [19] BALOOCH, M. and OLANDER, D. R., J. Chem. Phys. 63, 4772 (1975).
- [20] SEGAL, H., RICHARDS, T. G., Adv. Cryogenic Engineering (Academic Press, 1975.) Vol. 21.
- [21] CONN, R. W., GOHAR, Y., MAYNARD, C. W., Trans. Amer. Nucl. Soc. 22, 12 (1976).
- [22] CLEMMER, R. G., LARSEN, E. M., WITTENBERG, L. W., Nucl. Eng. and Design (1976) (in press).
- [23] MICHEL, D. J., SERPAN, C. Z., SMITH, H. H. and PIEPER, A. G., Nucl. Technol. 22, 79, (1974).
- [24] KINGSBURG, F. D. and MOTEFF, J., Trans. Amer. Nuc. Soc., 12, 575, 1969.  
See also, MOTEFF, J. AND KINGSBURG, F. D., Trans. Amer. Nuc. Soc., 10, 428, (1967).
- [25] GRAY, W. J., MORGAN, W. C. and TINGEY, G. L., Battelle Northwest Lab. Report, BNWL-2078 (June, 1976.)
- [26] MILLS, R. G., ed. "A Fusion Power Plant." Princeton Plasma Physics Lab. Report, MATT-1050 (1974).
- [27] SZE, D. K., LARSEN, E. M., CHENG, E. T., CLEMMER, R. G., "A Gas Carried Li<sub>2</sub>O Cooling-Breeding Fusion Reactor Blanket Concept," Nucl. Eng. Dept. Report, UWFD-151, (Univ. of Wisconsin, July, 1975).
- [28] BLOOM, E. E., WIFFEN, F. W., MAZIASZ, P. J. AND STIEGLER, J. O., "Temperature and Fluence Limits for a Type 316 Stainless Steel First Wall," Nucl. Technol. (in press).

Table 1Major Characteristics and Parameters of UWMAK-IIIa. General Features

Structural Material	Mo Alloy, TZM
Coolant	
Inner Blanket	He
Outer Blanket	Lithium (natural)
Shield	He
Fuel Cycle	(D-T), Li
Total Tritium Inventory	35.8 kg
Power Cycle	
Blanket	Closed Cycle He
Divertor	Na-Steam
Thermal Power During Burn	5000 MW(th)
Average Thermal Power	4735 MW(th)
Average Electrical Power	1985 MW(e)
Net Plant Efficiency	41.9%

b. Plasma Characteristics

Major Radius	8.1 m	Plasma Current	15.8 MA
Plasma Radius	2.7 m	Poloidal Beta	2.2
Shape Factor	1.6	Total Beta	~9%
Height to Width		q(o)	~1.0
Ratio	~2	q (near separatrix)	~3.5
Plasma Shape	"Triangular D"	Current Rise Time	15 s
Magnetic Axis	9.0 m	Plasma Burn Time	1800 s
Plasma Heating		RF Power	40 MW
Method	RF	Toroidal Field Ripple	~1%
RF Frequency	60 MHz		
Mode	Fast Magneto-sonic Wave		
Impurity Control Method - Double Null Divertor + Low Z Liner			

c. Blanket Performance Characteristics (R-Z Toroidal Neutronics)

Breeding Ratio	1.25	Max. Temp. in TZM	1000°C
Average Neutron		Max. Temp. in Li	980°C
Wall Loading	2.5 MW/m <sup>2</sup>	Max. Temp. in He	870°C
Total Energy Per		Tritium Inventory	1.0 kg
Fusion	20.1 MeV		

d. Magnet Parameters

Number of Toroidal Field Magnets	18
Magnet Superconductor	NbTi
Maximum Field	8.75 T
On Axis Magnetic Field	4.05 T
Magnet Stabilizer	Al
Magnet Structure	Al Alloy, 2219
Horizontal Bore	12.75 m
Vertical Bore	24.08 m
Energy Stored in Toroidal Field	108 GJ

Table 2

UWMAK-III Reactor Cycle

<u>Time (Sec.)</u>	
0-15	<u>Startup</u> : Plasma and divertor currents rise to full value; transformer currents begin to drop.
15-30	<u>RF Heating</u> : Plasma and divertor currents at full value; transformer currents continue to drop.
30-1830	<u>Burn</u> : Transformer currents drop to maximum negative value.
1830-1850	<u>Shutdown</u> : Plasma and divertor currents drops to zero; transformer currents rise to provide negative startup flux.
1850-1890	<u>Pumpout and recharge</u> : First 20 seconds hydrogen gas pumped into cool plasma, residual gas pumped out. Final 20 seconds; transformer currents reset to initial values.
1890-1900	<u>Final pumpout and refill</u> : Chamber purged and refilled with fresh fuel.

Figure Captions

- Fig. 1 Cross section view of nuclear island design for UWMAK-III.
- Fig. 2 Plan view of building arrangement for a reactor such as UWMAK-III. Note that the area and volumes are, within 20%, about the same as for the Clinch River Fast Breeder Reactor [8].
- Fig. 3 Comparison of the plasma and toroidal field coils in UWMAK-II [3,4] and UWMAK-III illustrating the sharp reduction in size.
- Fig. 4 Schematic illustration of the blanket and shield design for UWMAK-III. Tritium breeding is only in the outer blanket.
- Fig. 5a Variation of the neutron wall loading with poloidal angle.  
b. Variation of the helium production rate and atom displacement rate in the first structural wall of TzM.
- Fig. 6 A comparison of estimated costs for a UWMAK-III type reactor with other non-fuel-limited future energy sources. Costs for all other systems were developed by the Bechtel Corp. The perspective is that while improvements are clearly required, the UWMAK-III costs are similar to those estimated for other advanced technologies, and not appreciably greater.

# CROSS SECTION VIEW OF UWMAK III

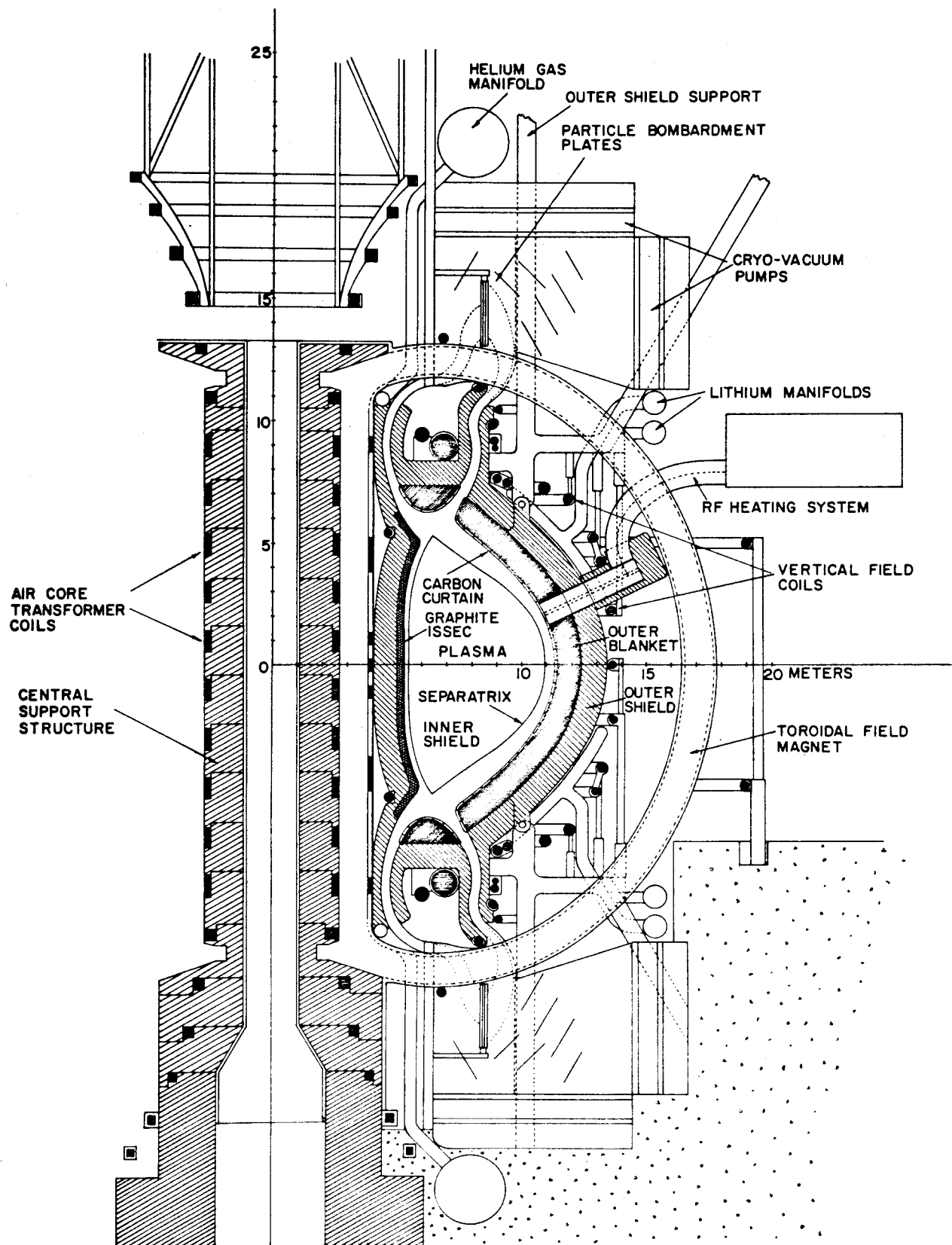
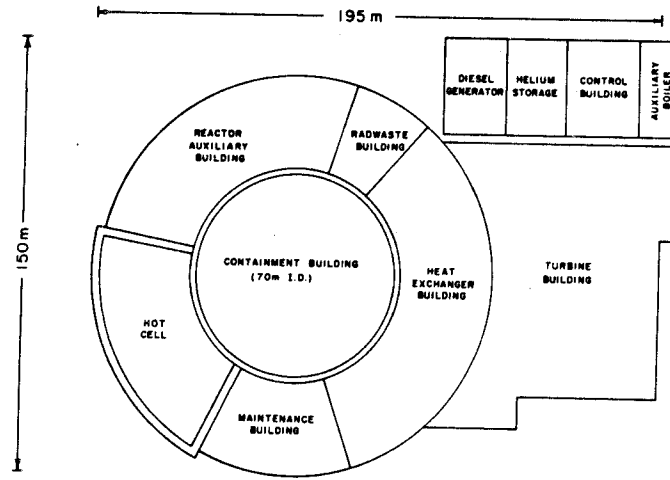


Figure 1



UWMak-III PLAN VIEW

Figure 2

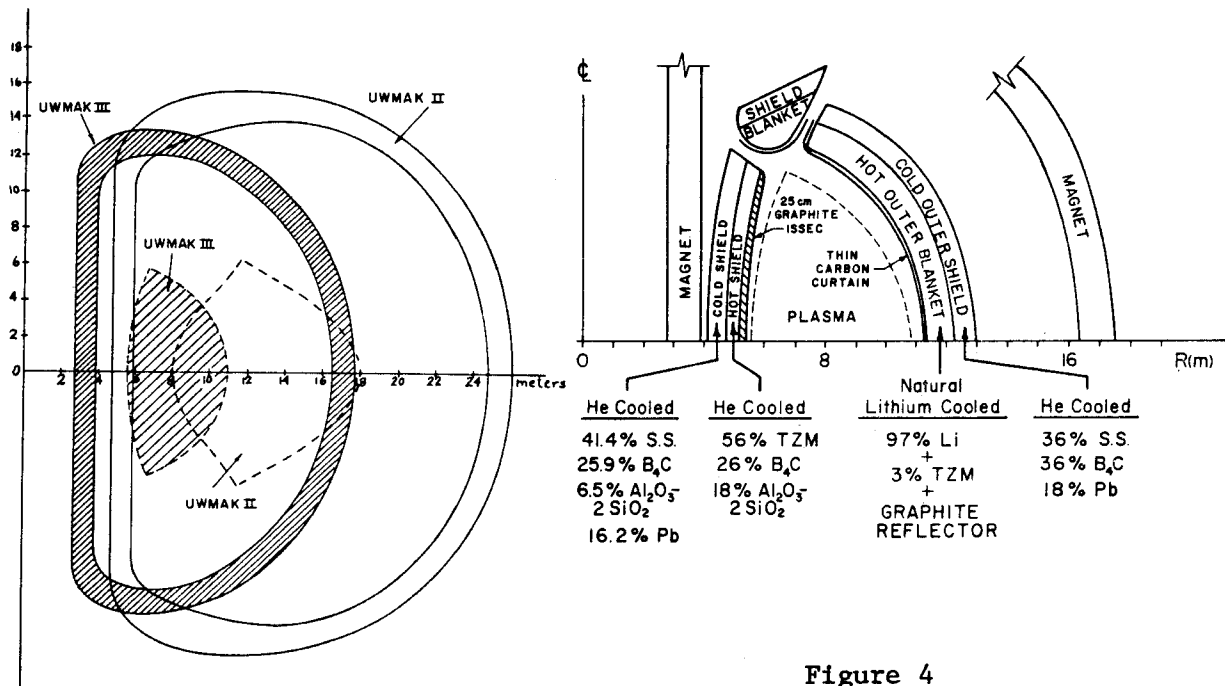


Figure 3

Figure 4

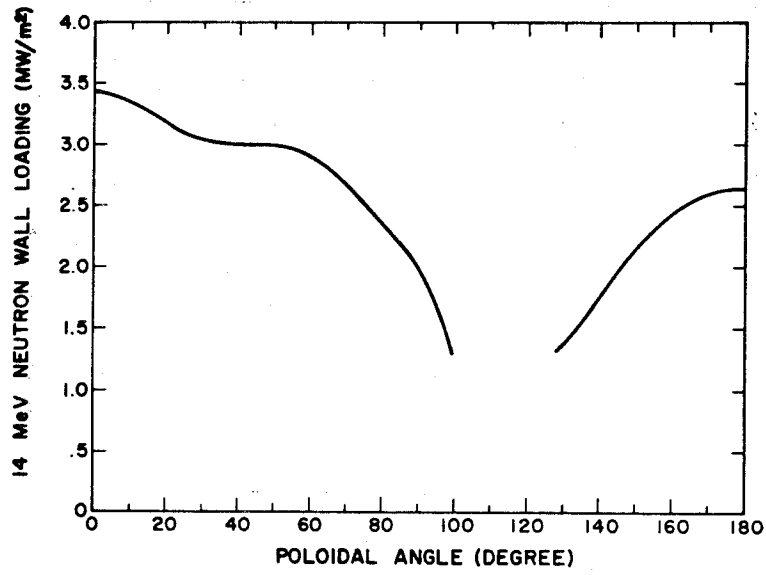


Figure 5a

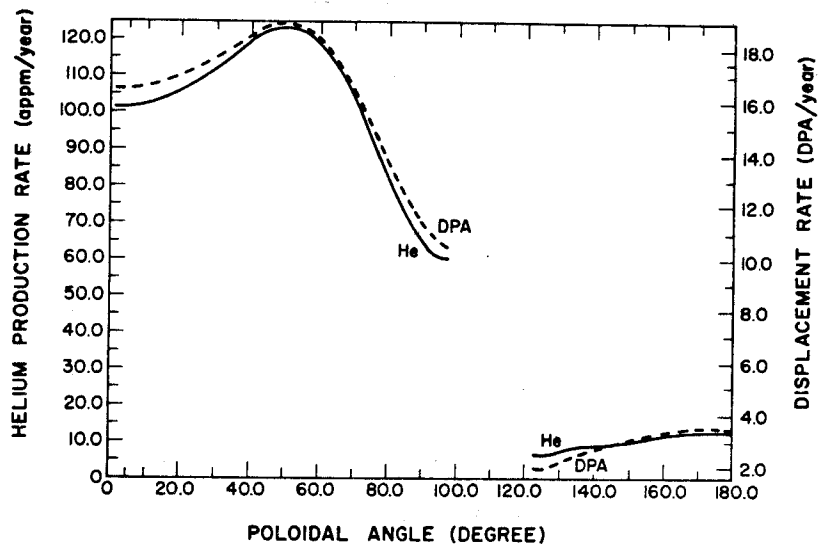


Figure 5b



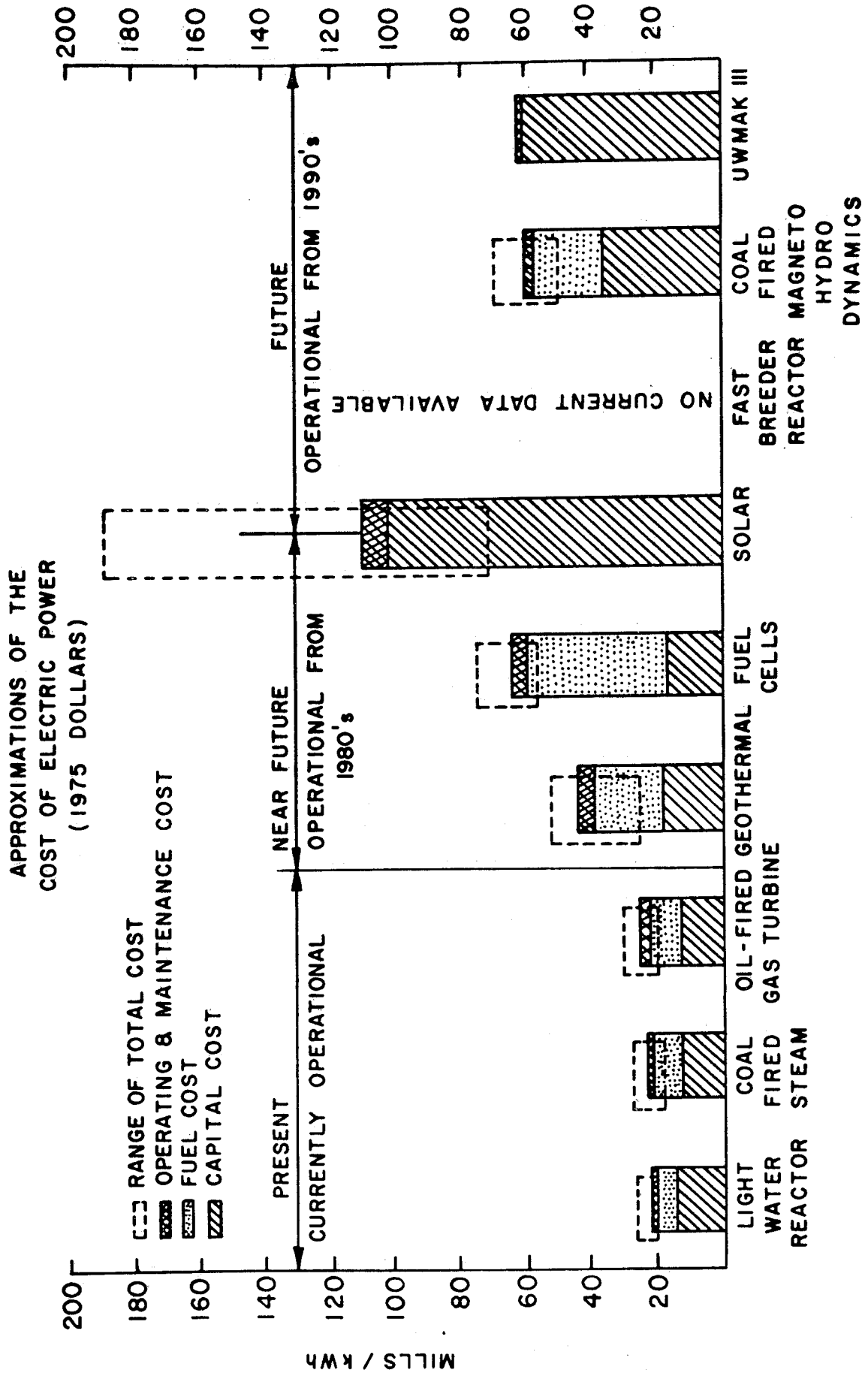


Figure 6